

## EROSION OF A GEOPOLYMER

K.C. Goretta<sup>†</sup>, Nan Chen<sup>†</sup>, J.L. Routbort<sup>†</sup>, G.C. Lukey<sup>‡</sup>, and J.S.J. van Deventer<sup>‡</sup>

<sup>†</sup>*Energy Technology Division, Argonne National Laboratory, Argonne, Illinois 60439-4838, USA. E-mail: routbort@anl.gov*

<sup>‡</sup>*Department of Chemical Engineering, The University of Melbourne, Victoria 3010, AUSTRALIA. E-mail: jsj.van\_deventer@chemeng.unimelb.edu.au*

### ABSTRACT

**Solid-particle erosion studies were conducted on a representative geopolymer. The test conditions were normal impact of 390- $\mu\text{m}$  angular  $\text{Al}_2\text{O}_3$  erodent particles moving at 50, 70, or 100 m/s. Steady-state erosion rates were obtained and the material-loss mechanism was studied by scanning electron microscopy. The geopolymer responded as a classic brittle material. Elastic-plastic indentation events led to formation of brittle cleavage cracks that resulted in spallation of material. The erosion rate was proportional to erodent velocity to the 2.3 power. The erosion rate and mechanism for the geopolymer were nearly identical to what has been observed for erosion of Si single crystals.**

*Keywords: geopolymer, erosion, fracture*

### 1. INTRODUCTION

Geopolymeric materials have been applied successfully to stabilization and solidification of many waste materials (Campbell *et al.*, 1987; Comrie, 1988; Davidovits *et al.*, 1990; Van Jaarsveld *et al.*, 1998 and 1999). For encapsulation of heavy metals, however, most systems currently used are based on Portland cement (Hills *et al.*, 1993; Conner, 1993) or, in some cases, phosphate cements (Wagh *et al.*, 1999; Singh *et al.*, 1997). Depending on the product,

mechanical properties of the various final forms may be of concern. For example, abrasion, water-erosion, solid-particle-erosion, and fracture studies have been conducted on various Portland and phosphate cements (Fwa and Low, 1990; Momber and Kovacev, 1994; Goretta *et al.*, 1999a,b).

Geopolymers generally contain less porosity than cements, and superior mechanical properties may therefore be expected (Davidovits, 1991). We have previously subjected Portland and phosphate cements and many other engineering materials to erosion by streams of angular Al<sub>2</sub>O<sub>3</sub> particles (Routbort, 1996). In this study, we have conducted identical tests on a representative geopolymer and then compared the resulting data set with those from other studies. The goal was to establish the extent to which geopolymers respond to erosion as do cements or conventional ceramics.

## **2. EXPERIMENTAL PROCEDURES**

### **2.1. Geopolymer synthesis and specimen fabrication**

[Grant to provide]

Densities were determined geometrically. The average specimen for strength testing was tested in the as-formed condition. Specimens for erosion testing were cut from the billet with a diamond-bladed saw. The average specimen for determination of erosion rate was  $\approx 3 \times 19 \times 25$  mm. No surfaces were polished. Smaller specimens were also prepared for study of individual impact sites (Routbort, 1996). These were polished with 1- $\mu$ m diamond paste.

### **2.2. Erosion testing**

The curing strength of the geopolymer was monitored with a penetrometer. In addition, several cylinders were subjected to standard concrete compressive tests in a hydraulic press. The force was applied at a rate of  $20 \pm 2$  MPa/min until the specimen failed.

Solid-particle erosion tests were carried out in a slinger-type apparatus that has been described previously (Routbort, 1996, and references therein). Tests were conducted in

vacuum ( $\approx 500$  mTorr), and so aerodynamic effects were negligible. The feed rate of the erodent was  $\approx 8$  g/min. At such a slow rate, interactions between particles were also negligible. Consistent and reproducible measurements could therefore be made.

The erodent particles were angular  $\text{Al}_2\text{O}_3$  abrasives (Norton Alundum 38) with mean diameter of  $390 \mu\text{m}$  (Routbort, 1996). The particle velocity ( $V$ ) was 50, 70, or 100 m/s and the angle of impact was  $90^\circ$ . All eroded surfaces were approximately  $19 \text{ mm} \times 19 \text{ mm}$ . Steady-state erosion rates (ER, in mg/g) were determined from plots of the specimen weight loss versus weight of particles impacting the surface. At least five runs were conducted for each specimen. To avoid possible problems due to environmental effects such as adsorption of water, each experiment to determine the ER values was completed in one day. Following each run, specimens were removed, brushed, cleaned by an air blast, and weighed. Each cycle of specimen removal through weighing took  $14 \pm 2$  min. It is estimated that the average weight-loss measurements were accurate to  $\pm 5\%$ . Uncertainties arose due to incomplete cleaning of the surfaces and slight adsorption of water.

Scanning electron microscopy (SEM) observations were made to correlate damage morphology of the eroded surfaces with the weight-loss and strength measurements. Single-impact damage sites were also examined by SEM.

### **3. RESULTS AND DISCUSSION**

#### **3.1. Geopolymer results**

The geopolymer appeared to contain limited porosity. Its average density was  $2.1 \text{ g/cm}^3$ . Its average strength was 35 MPa, which is on the low side of what we typically produce.

Representative data for weight loss versus dose of impacting particles are shown in Fig. 1. ER was defined as the slope of the linear least-squares fit to the data. The scatter in the data for duplicate specimens tested at 70 and 100 m/s was probably more attributable to specimen differences than difficulty with making reproducible measurements. For example, two different heats of Ni metal, tested on our slinger apparatus 15 years apart, yielded ER values within less than 2% of each other.

Erosion rate versus velocity of impacting particles is shown in Fig. 2. For brittle materials,  $ER \propto V^n$ , where the value of  $n$  depends on choice of model and shape of the impacting particle (Routbort, 1996). In the model of Weiderhorn and Lawn (1979), which is based on quasi-static impacts of sharp indenters,  $n = 2.4$ . For the geopolymer tested here,  $n = 2.3 \pm 0.2$ , with the error bars comprising estimates of uncertainty inherent in making the measurements and the quality of the statistical fits to the data.

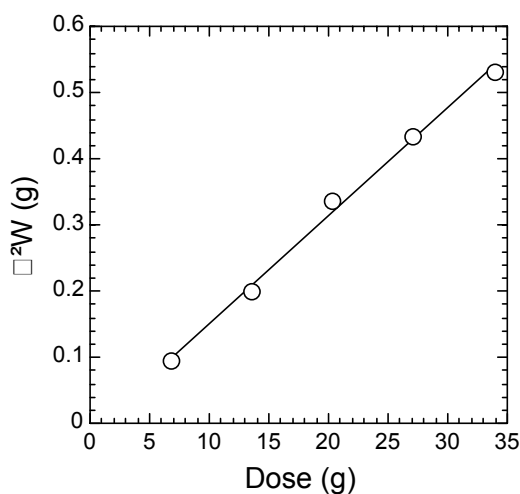


Figure 1: Weight loss vs. erodent dose for geopolymer impacted at 90° and 70 m/s.

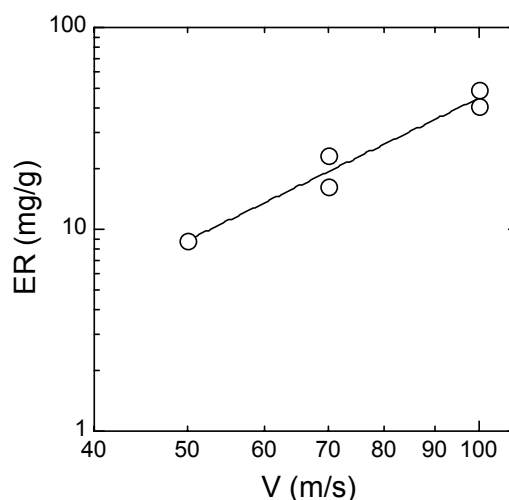


Figure 2: Steady-state erosion rate vs. velocity for geopolymer impacted at 90°.

The data yielded consistent ER values and a dependence of ER on  $V$  as predicted by Weiderhorn and Lawn (1979). As such, the geopolymer appeared to respond as an ideal brittle material. SEM observations were also consistent with erosion of a classically brittle ceramic. In brittle solids, material loss induced by solid-particle impact is a sequential event. In brief: (1) Indentation creates an elastic-plastic zone beneath the impacting particle. (2) A radial crack perpendicular to the specimen surface is created beneath the elastic-plastic zone. (3) As the erodent particle recoils, a resulting tensile stress state induces formation of a lateral cracks approximately parallel to the surface. (4) The lateral cracks propagate to the surface and a chip spalls off.

The single-impact sites were characteristic of erosion of a brittle solid. Two basic types of events were observed. Some of the impacts evinced all of the features that lead to material

removal: indenting, radial-crack formation, and spalling caused by propagation of lateral cracks (Fig. 3a). Most impact sites were similar, but no lateral crack had propagated sufficiently to allow for removal of significant material (Fig. 3b). As expected, the size of the damage site scaled with velocity of impact. The microstructure between impact sites was dense and rather uniform, but contained many small cracks. These cracks may be responsible for the relatively low strength of the geopolymer.

Figure 3: SEM photomicrographs of normal-incidence single-impact sites in the geopolymer: (a)  $V = 50$  m/s and (b)  $V = 100$  m/s.

The steady-state erosion surfaces were as would be expected from the data and the single-impact observations. The surfaces were rough, and overlapping brittle cleavage fractures were evident. In addition, indentation events (Fig. 4a), which contained indications of plastic flow (Fig. 4b), were prevalent. Small pieces of  $Al_2O_3$  were scattered over the surface eroded at 100 m/s, which indicates that the erodent fragmented to some extent during impact.

The dominant features that emerged during the SEM were the inherent uniformity and high density of the geopolymer and the large cleavage fractures that were induced during the steady-state erosion testing. Such large-scale fracturing is characteristic of materials of low fracture toughness.

Figure 4. SEM photomicrographs of geopolymer eroded into steady state at 100 m/s: (a) representative region, in which brittle fracture and indenting are observed, and (b) evidence for plastic flow within an indentation site.

### 3.2. Comparison with other engineering materials

Our slinger apparatus for erosion testing has been used since 1975. No significant modifications have been made. Because test conditions have remained constant, direct comparisons of data sets are possible. Comparisons with results from others can be made, but the conditions are almost never identical and so it can be difficult to draw unequivocal conclusions (Routbort and Scattergood, 1992). We have therefore restricted our comparison of the erosion rate of the geopolymer to results from other materials tested on our apparatus. Materials that have been tested include metals, ceramics, cements, polymers, and composites. Data for a single set of conditions (erodent = 390- $\mu\text{m}$  angular  $\text{Al}_2\text{O}_3$ , impact at  $90^\circ$ ,  $V = 100$  m/s) are displayed in Fig. 5. The data are expressed as weight of material lost rather than volume of material lost. Densities ranged from 1.33  $\text{g}/\text{cm}^3$  for the bismaleimide polymer (Brandstatter *et al.* (1991) to 7.93  $\text{g}/\text{cm}^3$  for the 304 stainless steel (Goretta *et al.* (1991).

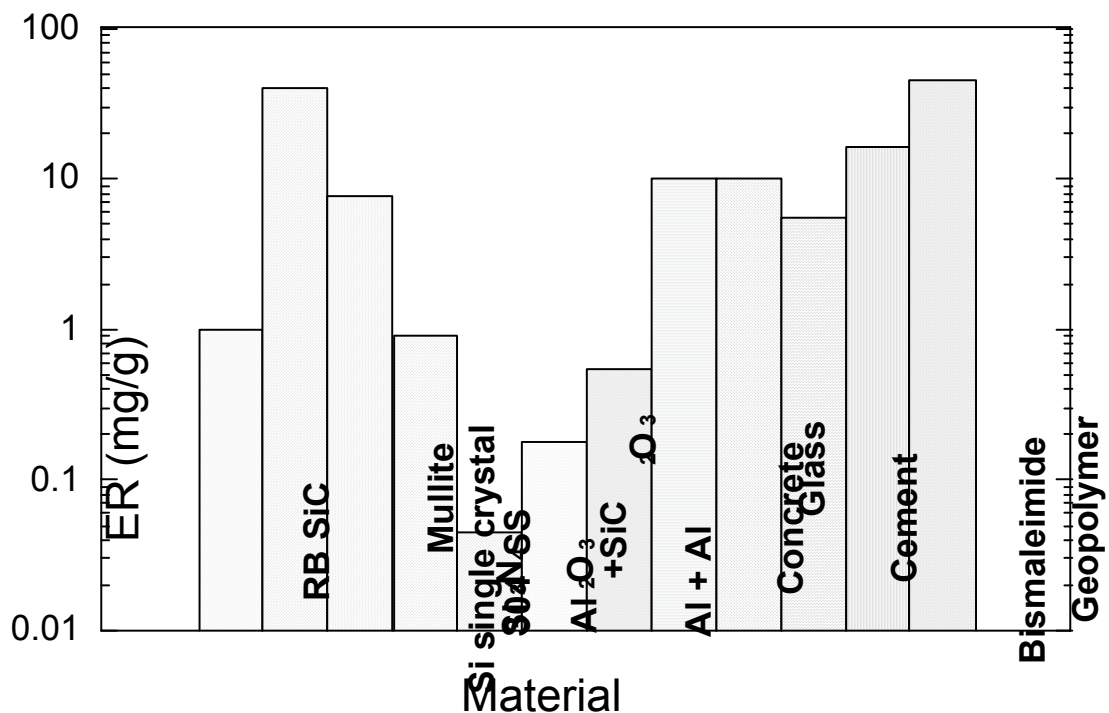


Figure 5: Erosion rates of various engineering materials impacted at normal incidence by 390- $\mu\text{m}$  angular particles with  $V = 100$  m/s. Data taken from Routbort *et al.* (1980), Routbort and Scattergood (1980), Morrison *et al.* (1985), Morrison *et al.* (1986), Morrison *et*

*al.* (1987), Routbort *et al.* (1990), Goretta *et al.* (1999a), Brandstädter *et al.* (1991), and this study; in some cases, minor interpolation or extrapolation was required.

The erosion of the geopolymer was closest to that of Si single crystals. The erosion mechanism was probably closest as well. For both materials, classic brittle fracture occurred, with little or no evidence of a toughening mechanism mitigating the fracture. This result is mildly surprising. It offers testament to the relative density and phase purity of the geopolymer. It also provides guidance as to how erosion resistance can be improved, should that prove to be necessary. Geopolymers are simple and easy to produce and they readily lend themselves to incorporation into various composites. Such composites exhibit improved fracture toughness (Hammell *et al.*, 1998) and should prove to be more erosion resistant than an unreinforced geopolymer. Future work should include examination of the response of composite geopolymers to erosion.

The geopolymer is most similar to Portland cement in terms of synthesis and application. Although the erosion rate of Portland cement (Goretta *et al.*, 1999a) was similar to that of the geopolymer, the mechanisms were quite different. Whereas the geopolymer evinced material loss by classic brittle fracture, material loss in the Portland cement occurred by smaller-scale fractures coupled with effects of material degradation caused by loss of water. Local heating caused by the kinetic energy of the impacts induced the heating.

#### **4. SUMMARY**

Solid-particle erosion studies were conducted at normal incidence and 50-100 m/s on a representative geopolymer. The geopolymer responded as a classic brittle material. Elastic-plastic indentation events led to formation of brittle cleavage cracks that resulted in spallation of material. The erosion rate was proportional to erodent velocity to the 2.3 power, which is in agreement with predictions of Weiderhorn and Lawn (1979). The geopolymer exhibited evidence of low fracture toughness and thus relatively high erosion rate compared with other engineering materials.

#### **ACKNOWLEDGMENTS**

The work at Argonne National Laboratory was supported by the U.S. Department of Energy, under Contract W-31-109-Eng-38.

## REFERENCES

Brandstädter, A, Goretta, K C, Routbort, J L, Groppi, D P and Karasek, K R, 1991. Solid-particle erosion of BMI polymers, *Wear*, 147:155-164.

Campbell, K M, El-Korchi, T, Gress, D and Bishop, P, 1987. Stabilisation of cadmium and lead in Portland cement paste using a synthetic seawater leachant, *Environmental Progress*, 6:99-103.

Comrie, D C, 1988. New hope for toxic waste, *The World and I*, pp. 171-177.

Conner, J R, 1993. Stabilizing hazardous waste, *Chemtech*, pp. 35-44.

Davidovits, J, 1991. Geopolymers: Inorganic polymeric new materials, *Journal of Thermal Analysis*, 37:1633-1656.

Davidovits, J, Comrie, D C, Paterson, J H and Ritcey, D J, 1990. Geopolymeric concretes for environmental protection, *Concrete International*, 12:30-40.

Fwa, T F and Low, E W, 1990. Laboratory evaluation of wet and dry abrasion resistance of cement mortar, *Cement, Concrete, and Aggregates*, 12:101-106.

Goretta, K C, Arroyo, R C, Wu, C-T and Routbort, J L, 1991. Erosion of work-hardened copper, nickel, and 304 stainless steel, *Wear*, 147:145-154.

Goretta, K C, Burdt, M L, Cuber, M M, Perry, L A, Singh, D, Wagh, A S and Routbort, J L, 1999a, Solid-particle erosion of Portland cement and concrete, *Wear*, 224:106-112.

Goretta, K C, Singh, D, Tlustochowicz, M, Cuber, M M, Burdt, M L, Jeong, S Y, Smith, T L, Wagh, A S and Routbort, J L, 1999b. Erosion of magnesium potassium phosphate



ceramic waste forms, *Materials Research Society Symposium Proceedings*, 556:1253-1260.

Hammell, J, Balaguru, P and Lyon, R, 1998. Influence of reinforcement types on the flexural properties of geopolymer composites, *SAMPE Proceedings*, 43:1600-1608.

Hills, C D, Sollars, C J and Perry, R, 1993. Ordinary Portland cement based solidification of toxic waste: The role of OPC reviewed, *Cement and Concrete Research*, 23:196-212.

Momber, A and Kovacevic, R, 1994. Fundamental investigations on concrete wear by high velocity water flow, *Wear*, 177:55-62.

Morrison, C T, Routbort, J L and Scattergood, R O, 1985. Solid-particle erosion of mullite, *Wear*, 105:19-27.

Morrison, C T, Routbort, J L and Scattergood, R O, 1987. Erosion of SiC whisker reinforced silicon nitride, *Materials Research Society Symposium Proceedings*, 78:207-214.

Morrison, C T, Scattergood, R O and Routbort, J L, 1986. Erosion of 304 stainless steel, *Wear*, 111:1-13.

Routbort, J L, 1996. Degradation of structural ceramics by erosion, *Journal of Nondestructive Evaluation*, 15:107-112.

Routbort, J L, Helberg, D A and Goretta, K C, 1990. Erosion of whisker-reinforced ceramics, *Journal of Hard Materials*, 1:123-135.

Routbort, J L and Scattergood, R O, 1980. The erosion of silicon single crystals, *Journal of the American Ceramic Society*, 63:635-640.

Routbort, J L and Scattergood, R O, 1992. Solid-particle erosion of ceramics and ceramic composites, in *Erosion of Ceramic Materials* (Ed. Ritter, J E), pp. 23-51 (Trans Tech. Publications: Geneva, Switzerland).

Routbort, J L, Scattergood, R O and Turner, A P L, 1980. Erosion of reaction-bonded silicon carbide, *Wear*, 59:363-375.

Singh, D, Wagh, A, Cunnane, J and Mayberry, J, 1997. Chemically bonded phosphate ceramics for low-level mixed-waste stabilization, *Journal of Environmental Science and Health*, A32: 527-541.

Van Jaarsveld, J G S, Van Deventer, J S J and Lorenzen, L, 1998. Factors affecting the immobilisation of metals in geopolymerised fly ash, *Metallurgical and Materials Transactions B*, 29:283-291.

Van Jaarsveld, J G S, Van Deventer, J S J and Schwartzmann, A, 1999. The potential use of geopolymeric materials to immobilise toxic metals: Part II. Material and leaching characteristics, *Minerals Engineering*, 12:75-91.

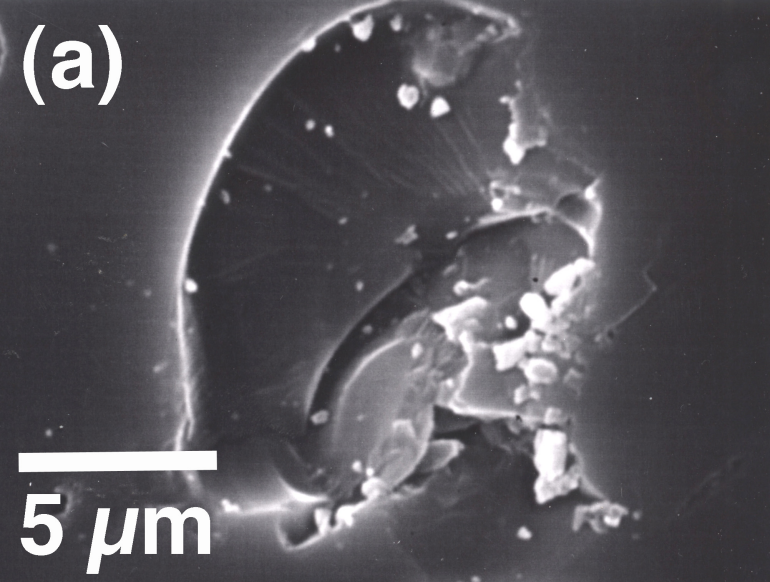
Wagh, A, Strain, R, Jeong, S Y, Reed, D, Krouse, T and Singh, D, 1999. Stabilization of Rocky Flats Pu-contaminated ash within chemically bonded phosphate ceramics, *Journal of Nuclear Materials*, 265:265-307.

Wu, W, Goretta, K C and Routbort, J L, 1992. Erosion of 2014 Al/particulate ceramic composites, *Materials Science and Engineering A*, 151:85-95.

The submitted manuscript has been created by the University of Chicago as Operator of Argonne National Laboratory ("Argonne") under Contract No. W-31-109-ENG-38 with the U.S. Department of Energy. The U.S. Government retains for itself, and others acting on its behalf, a paid-up, nonexclusive, irrevocable worldwide license in said article to reproduce, prepare derivative works, distribute copies to the public, and perform publicly and display publicly, by or on behalf of the Government.

**(a)**

**5  $\mu\text{m}$**

This scanning electron micrograph (SEM) shows a cross-section of a biological structure, possibly a seed or fruit. The structure is roughly semi-circular and contains several internal chambers or seeds. The surface is highly textured and appears to be covered in small, irregular particles or debris. A white scale bar is located in the bottom left corner, with the text "5 μm" below it. The label "(a)" is in the top left corner.

**(b)**



**25  $\mu\text{m}$**

This scanning electron micrograph (SEM) shows a fractured surface of a material. The fracture surface is highly irregular and jagged, with numerous small, bright, angular particles or debris scattered across it. The background is dark, and the overall appearance is that of a brittle fracture. A white horizontal scale bar is located in the bottom right corner, with the text '25 μm' written below it.

**(a)**



**25  $\mu\text{m}$**

This scanning electron micrograph (SEM) shows a highly textured, layered material. The surface is composed of numerous overlapping, irregularly shaped plate-like structures, likely lamellae or flakes, which are oriented in various directions. The overall appearance is that of a fractured or delaminated layered material. A white horizontal scale bar is located in the lower-left quadrant, with the text '25 μm' positioned directly below it.

**(b)**

  
**2  $\mu\text{m}$**

